Investigation of Creepage Distances on Printed Circuit Boards for Avionic Applications

Hendrik Schefer[1,3], Zhongqing Xu[1], Tobias Kopp[2,3], Regine Mallwitz[1,3], Michael Kurrat[2,3]
INSTITUTE FOR ELECTRICAL MACHINES, TRACTION AND DRIVES (IMAB)[1]
INSTITUTE FOR HIGH VOLTAGE TECHNOLOGY AND POWER SYSTEMS (elenia)[2]
CLUSTER OF EXCELLENCE SE²A – SUSTAINABLE AND ENERGY-EFFICIENT AVIATION[3]
TU Braunschweig
Braunschweig, Germany
Email: h.schefer@tu-braunschweig.de
URL: `https://www.tu-braunschweig.de/imab`
URL: `https://www.tu-braunschweig.de/elenia`
URL: `https://www.tu-braunschweig.de/se2a`

Acknowledgments

This work was supported by the Deutsche Forschungsgemeinschaft (German Research Foundation, DFG) through the Germany's Excellence Strategy-EXC 2163/1-Sustainable and Energy Efficient Aviation under Grant 390881007.

Keywords

≪Insulation≫, ≪Reliability≫, ≪HVDC≫, ≪High voltage power converters≫, ≪Aerospace≫

Abstract

Avionic power electronic applications need enormous power densities ($10\,\frac{\mathrm{kW}}{\mathrm{kg}} <$) under high reliability to enable a high level of electrification. An increase in the DC bus voltage and high switching frequencies due to WBGs is unavoidable. An improved level of integration of these WBGs is needed to meet the aviation specific requirements regarding weight. Thus, this paper focuses on determining the breakdown voltage induced by DC voltages on printed circuit boards to show new design possibilities for future .

I Introduction

The electrification of aerospace is one opportunity to fulfil societal goals to reduce CO_2 emissions, for example, European Flightpath 2050. Power electronics in aircraft are subject to challenging requirements[1]. The conventional drive train must be replaced by electrical components and withstand environmental conditions in flight heights up to 13.000 m. For a sufficient overall design which considers in particular functional safety and to exhaust all opportunities of an electrical drive train, the power electronic should not be dependent on air-conditioning [1].
In the last decade, wide-bandgap semiconductors have offered new technology approaches to increase the bus voltage (up to 7.5 kV) at high switching frequencies (20 kHz <) and high efficiencies in mobile power applications. Due to the high switching frequencies at higher powers, passive components gain an enormous weight reduction compared to conventional semiconductors, especially magnetics profit. Magnetics are needed as filter compounds in drives or DC/DC converters connecting batteries or fuel cells. Furthermore, higher junction temperatures enable further advantages in near future [1].
A compact design requires deep knowledge about insulation coordination in power dense avionic power electronics under challenging environmental conditions. Therefore, the application of the well-known

Paschen's law is questionable for creepage distances, due to the gas-solid interface and its influence on the breakdown voltage. This paper focuses on determination of the breakdown voltage induced by DC voltages on printed circuit boards (PCBs). It research the dielectric basis and is thus crucial for further studies, for example to understand the ageing of creepage distances due to high dynamic rectangular voltage shapes ($\frac{du}{dt}|_{\max} > \frac{60\,\text{kV}}{\mu\text{s}}$).
There are also standards, for example for equipment connected to low voltage systems, IEC 60 664 "Insulation coordination for equipment within low-voltage supply systems", which includes considerations of altitudes up to 2000 m, DC voltages up to 1500 V, AC rated voltage of 1000 V, sine wave frequencies up to 30 kHz, the Comparative Tracking Index (CTI) and different pollution degrees. Creepage distances from the IEC 60 664 are often used for electric vehicles [2]. Other standards like IEC 62368-1 [3] (Subsequent standard from IEC 60950 since 2020) have a similar restriction considering the voltage height of the voltage supply. High voltage standards like the IEC 60815 are specially designed for ceramic and glass insulators and are far away from the application of PCBs. In aviation, the MIL-HDBK-5400 is often used, but do not consider stresses of WBGs.
Thus, the higher the switching frequency, high voltages and shorter rise times, the more likely occur partial discharge. In publications [4], comparable investigations show interesting results and test bench ideas. This paper distinguishes the use of a Design of Experiments (DoE) to get a statistical significance and the preparation for rectangular stress in further studies. Other publications [5] and [6] pursue the same research objectives.
The paper is structured into an investigation methodology in section II, the description of the DoE in section III, test bench design in IV & VI, the data analysis in section V & VII and the conclusion in VIII.

II Methodology of Investigations

The International Standard Atmosphere [7] describes the environmental conditions over altitude. The humidity, pressure and temperature decrease with the altitude. Otherwise, the temperature inside the housing can reach higher values because of the losses and the high-required power density. Additional, outer conditions at sea level have to be taken into account. For example, landing, taxing and take-off are other interesting operation points. Airports, depending on their geographical location, have extremely various outer conditions. A housing can protect the power electronics for external conditions, like humidity, temperature and pressure. Power electronic integration in the fuselage of the propulsor, like the drive inverter, requires deep understanding. Tab. I and II compare the environmental conditions and test bench boundaries. The test benches cover the environmental requirements.

Table I: Environmental conditions

		Temperature °C	rel. Humidity %	Pressure $\frac{\text{N}}{\text{m}^2}$	Voltage V
Environmental	min	-56.50	1	61943	
	max	+150	90	101325	

Table II: Test bench boundaries [* climate control, ** temperature control, TB: test bench]

		Temperature °C	rel. Humidity %	Pressure $\frac{\text{N}}{\text{m}^2}$	Voltage V
Climate TB	min	-70** / +5*	10*		0
	max	+180** / +95*	95*		5000
Pressure TB	min			100	0
	max			101325	12000

By the literature review, a lot of factors could be identified which have an impact on the breakdown voltage induced by DC voltages. The study indicates the temperature, humidity, pressure, electrode distance, the existence of the solder resist and pollution. Therefore, the analysis requires massive tests, which the DoE can reduce.

III Design of Experiments (DoE)

DoE is a scientific method that reduces experimental errors and R&D costs by optimizing the DoE protocols, reducing experimental workload, and scientifically analyzing experimental results [8].
For the climate test, a design of experiments is used to reduce the number of trials. Otherwise, the pressure test is conducted with the single factor method (single varying of one parameter set, pressure, distance).

A Design of the Devices under Test (DUTs)

Tests can be done at small probes and in suitable test benches. PCB probes with two contact surfaces and different electrode distances/geometries offer good opportunities. The distances between the electrodes are available from 0.2 mm to 0.5 mm with and without solder resist. These PCBs are designed to have a breakdown in the limits of the voltage source and in future studies for accelerated altering due to rectangular voltage shapes. Fig. 1 shows examples of the designed Devices under Tests (DUTs). This study focuses on the breakdown voltage and serves primary data for the accelerated testing.

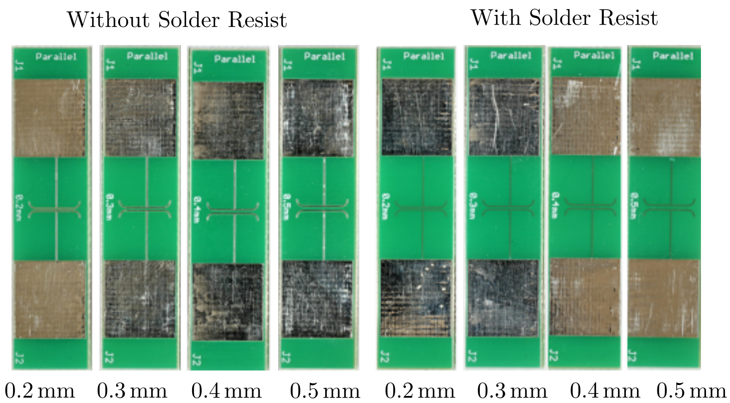

Fig. 1: DUTs with/without solder resist (0.2 mm to 0.5 mm) with the same geometry

B Factors of Climate Tests

The test bench has physical boundaries, as mentioned above in Tab. II in section II. For the presented studies, the number of factors is reduced. In the Tab. III below, the considered factors are given.

Table III: Factors of climate tests

Temperature T	rel. Humidity $r.H$	Distances d	Solder Resist
30 °C	30 %	0.2 mm	without
50 °C	55 %	0.3 mm	
70 °C	80 %	0.4 mm	
		0.5 mm	

C D-optimal Design of Experiments for Climate Tests

Compared with full factorial design, D-optimal design uses as few experiments as possible to obtain as much information as possible. In the experimental response model Eq. 1, the covariance of the x matrix is proportional to $(X'X)^{-1}$, so it needs to be minimized $(X'X)^{-1}$. The D-optimal can equate this problem to solving the determinant problem, i.e., maximizing $|X'X|$ [9]. The coefficients (β_0 to β_{11}) are output parameters of the DoE.

$$U_{\text{Break}} = \beta_0 + \beta_1 \cdot T + \beta_2 \cdot d + \beta_3 \cdot r.H + \beta_{11} \cdot T^2 + \varepsilon \tag{1}$$

The test matrix shown in Tab. IV is calculated and optimised using a data analysis software, called "Cornerstone". A randomised experimental design avoids systematic errors. The software is also helpful in evaluating the experiments.

Table IV: Output of the DoE (test matrix)

Nr.	T °C	$r.H$ %	d mm	Nr.	T °C	$r.H$ %	d mm
1.	30	55	0.2	8.	70	80	0.4
2.	50	55	0.4	9.	70	55	0.3
3.	70	30	0.4	10.	30	30	0.3
4.	70	30	0.2	11.	30	80	0.4
5.	50	80	0.2	12.	30	55	0.5
6.	50	30	0.5	13.	50	80	0.3
7.	70	80	0.5				

IV Climate Test Bench for Determining the Breakdown Voltage induced by DC voltages

As shown in Fig. 2, the breakdown experiments of the PCB specimen were carried out in the automated climate test bench. The computerised climate chamber test bench consists of a climate chamber, a HV source, real-time embedded industrial controller (Ni cRIO) and a test bench computer. A serial communication interface enables the controlling of the high voltage source and temperature and humidity of the climate chamber. For safety reasons, a contact switch shuts the voltage source down in case of an open door.

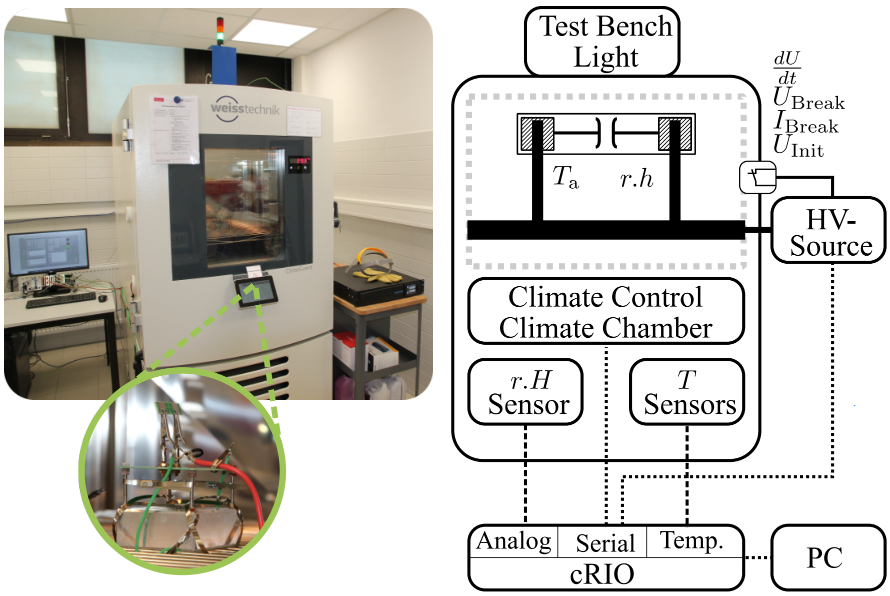

Fig. 2: Test Bench for realising climate factors

External sensors inside the climate chamber check the climate behaviour and enable capturing metadata. Crucial experimental test bench parameters are the voltage ramp, the threshold current (linked to carbonisation) and the initialisation voltage; therefore, the user can adjust these essential parameters in the graphical user interface.
After equipping the self-build HV interface, the climate test bench controls the environmental conditions (humidity and temperature) to the set values. The cRIO captures humidity, temperature, and time during the controlling time because the DUT faces the conditions from the beginning of the tests. After the predefined environmental conditions are reached, the voltage ramp starts. Getting the threshold condition (threshold current), the test bench stops, and the HV voltage supply switches off. Before exchanging the DUT, the user must determine the absence of voltage. The procedure begins from the starting point. The test bench is also designed for metadata analysis.
A pressure chamber can replace the climate chamber, which guarantees avionic pressure ranges (down to 1 mbar).

V Data Analysis of Climate Tests

The data originates from the test with the climate test bench. There are five and ten replicate experiments (Tab. V), and preliminary studies using data analysis with Matlab (Lilliefors) state a normal distribution. Due to the help of the standard deviation, it is noticeable that increasing the replicate experiments does not lead to better results at some measurement points. Especially the high humidity of $r.H = 80\,\%$ produces straying. However, a decrease in the standard deviation can be recognised at most of the measurement points.

Table V: Climate measurement data

	Five Replicate Experiments		Ten Replicate Experiments	
Nr.	$\overline{U}_{\text{Break}}$ /V	σ_U /%	$\overline{U}_{\text{Break}}$ /V	σ_U /%
1	1409.8	19.35	1440.7	15.58
2	2241.2	17.02	2209.9	11.99
3	2326	5.59	2302	6.23
4	1428.4	13.37	1497.6	12.29
5	935	6.2	992.9	11.08
6	2828.6	5.88	2920.5	5.52
7	1678.2	14.68	1674.7	15.53
8	1381.2	16.41	1339.1	11.81
9	1644.2	12.8	1724	11.94
10	1974	5.33	2000.7	6.86
11	1736	9.69	1701.6	11.39
12	2642	14.54	2625.7	11.14
13	1554.8	7.89	1450	14.4

The Tab. VI & VII illustrate the model parameter of $n = 5$ and $n = 10$. In comparing both models, an additional quadratic dependency of the temperature is added to the model ($n = 10$). Therefore, the temperature coefficient β_1 and the offset change in both models β_0.

Table VI: Model parameter (n=5)

β_0	β_1	β_2		β_3		β_{11}
V	$\text{V}\cdot\text{K}^{-1}$	mm	$\text{V}\cdot\text{mm}^{-1}$	%	$\text{V}\cdot\text{r.H}^{-1}$	$\text{V}\cdot\text{K}^{-2}$
2179	-6.50	0.2	-595.4	30	318.1	
		0.3	-129.2	55	91.5	
		0.4	195.7	80	-409.6	
		0.5	529.4			

Table VII: Model parameter (n=10)

β_0	β_1	β_2		β_3		β_{11}
V	$V \cdot K^{-1}$	mm	$V \cdot mm^{-1}$	%	$V \cdot r.H^{-1}$	$V \cdot K^{-2}$
993	46.13	0.2	-562.6	30	351.6	-0.516
		0.3	-148.1	55	117.1	
		0.4	176.7	80	-468.7	
		0.5	534			

The Tab. VIII expresses the fitting of the model to the captured data. As shown in Tab. VIII, for the PCB breakdown voltage predictive model ($n = 5$), the R^2 (goodness of fit in linear regression) is 0.9473, and the adjusted R^2 (corrected goodness of fit) is 0.8946. The RMSE (root mean square error) is 176.67; for the PCB breakdown voltage model ($n = 10$), R^2 is 0.9838, and the adjusted R^2 is 0.9611. Compared with the predictive model ($n = 5$), the PCB predictive breakdown voltage model ($n = 10$) has a better fit. Both R^2 of the deviation model of model ($n = 5$) and model ($n = 10$) are less than 0.6, and the deviation model fit is poor. However, the fit of the deviation model of model ($n = 10$) is slightly better than that of the predictive model ($n = 5$).

Table VIII: Goodness of fit [R^2: goodness of fit in linear regression, adjusted R^2: corrected goodness-of-fit, RMSE: root mean square error]

	Predictive PCB Breakdown Model			Deviation Model		
Model	R^2	adjusted R^2	RMSE	R^2	adjusted R^2	RMSE
$n = 5$	0.9473	0.8946	176.67	0.4916	0.3899	3.84
$n = 10$	0.9838	0.9611	108.32	0.5553	0.4663	2.36

Fig. 3 compares the predictive model ($n = 5$) with its confidence interval (98 %) with five fractional experiments to verify the quality of the model. Between different measurement values, a second order regression fits the data. The predictive model differs slightly from the fractional experiments; it can be recognised in the temperature dependency.

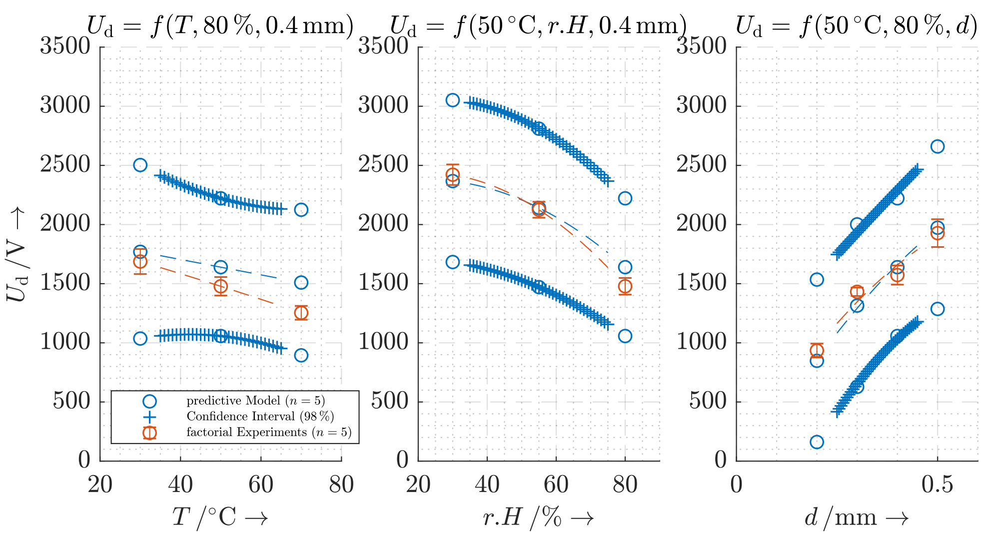

Fig. 3: Comparison fractional experiments vs. DoE predictive model ($n = 5$)

Fig. 4 evaluate the predictive model ($n = 10$) with its confidence interval (98 %) with the same five fractionals as in the study above. The five fractionals do not fit so well in the model ($n = 10$) as in the model ($n = 5$). The reason is the derivation of the fractional experiments. However, the derivation between both models is improved, as analysed in Tab. VIII, and a higher number of fractional tests will improve the derivation of the validating tests.

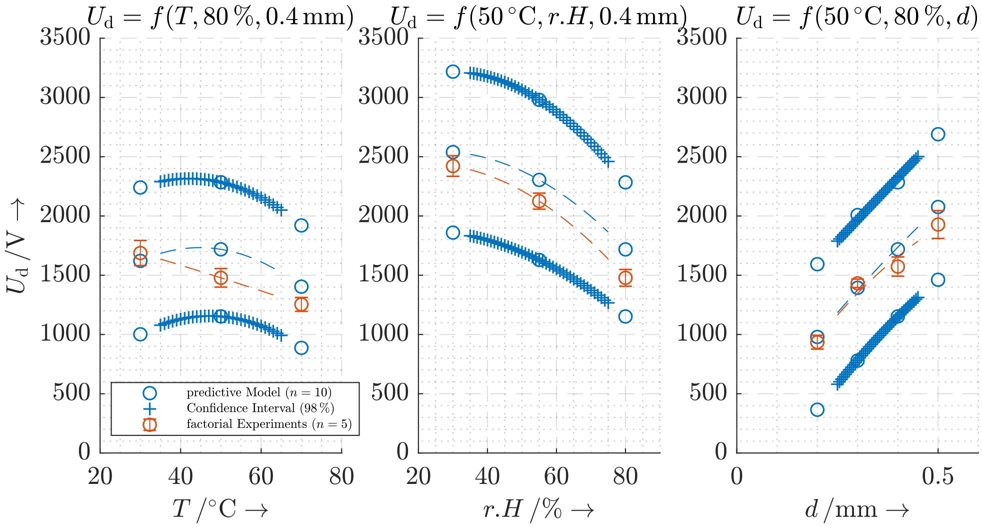

Fig. 4: Comparison fractional experiments vs. DoE predictive model ($n = 10$)

A Pareto analysis explains that distances have the most significant impact, second the humidity and third the temperature. A study with ten trials per test point offers a decrease in the derivation.

VI Pressure Test Bench for Determining the breakdown Voltage induced by DC voltages

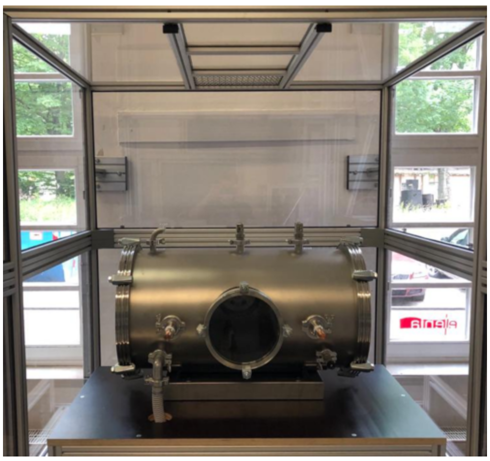

Fig. 5: Pressure chamber

A pressure chamber (Fig. 5) replaces the climate chest, which guarantees aeronautical pressure ranges (down to 1 mbar). The low-pressure chamber offers many features for insulation studies, such as high voltage bushings up to 12 kV (AC, DC) and high current bushings up to 400 A continuous and 5 kA peak. In addition, the low-pressure chamber has a viewing window made of borosilicate. This window makes the chamber suitable for analysing components using various optical methods such as spectrography or high-speed cinematography. Furthermore, the chamber is equipped with a large number of low voltage electrical bushings and several BNC bushings for required measurement equipment. Also, fluid feed-throughs are available.

VII Data Analysis of Pressure Test

During a meeting of the ETG department Q2 (German expert group for Materials, Insulation Systems, Diagnostics) in 2022 a demand for an improved knowledge of high voltage performance for creepage

distances in the pressure range of aviation was visible. Moreover standards like the IEC 62368-1 [3] only defines altitude dependencies for air gaps, a separate definition for creepage distances can be deduced from these values. However, these deduced values may not consider special breakdown behaviour of creepage distances for lower pressures.
As a contribution to the ongoing discussion, measurements of the creepage distance under a varied pressure will be presented within the pressure chamber, Fig 6. Currently, a combination with temperature and humidity will not be part of the results. The combination of these environmental conditions is challenging and still under development. It will be part of future investigations and is an important investigation target, as regarded in V.
Measurements of the breakdown voltage U_d were performed with the presented circuit board design (Fig. 6) using a DC Generator (Type: GLP1-g HV-DC 4 kV 10 mA, Company: Schleich GmbH).
For each data-point the breakdown voltage of 8 circuit boards were investigated. The here shown data represents the extended measurement uncertainty with a confidence interval of 98% of the first breakdown voltage of each PCB, Fig. 6.

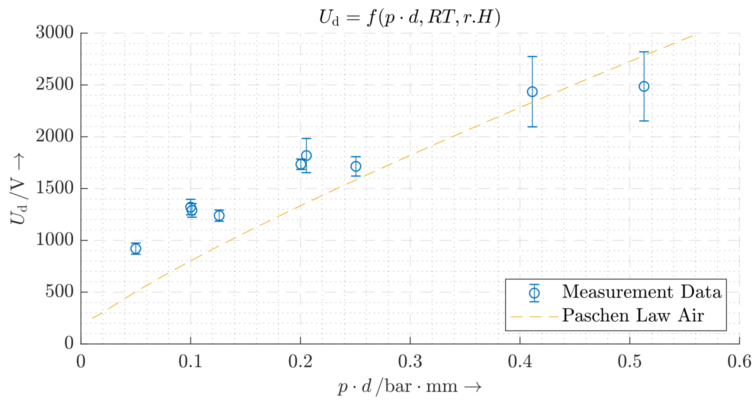

Fig. 6: Fractional pressure dependence breakdown-voltage for PCBs (T =room temperature, $r.H = 80\,\%$)

For this data analysis a single-factor research is done due to the relative small parameter area. The pressure is adjusted in the range of 1 bar, 0.5 bar and 0.25 bar to investigate an important area for the aviation. However, pressures down to 0.044 bar have to be tested according to [10]. Thus, this area should be integrated in future research. The gap distance on the PCB is chosen to 0.5 mm, 0.4 mm and 0.2 mm to match the measurements above, chapter 2.
In accordance with the well-known Paschen's law (dashed lines, Fig. 6) the x-Axis is the product of distance and pressure. The curve of Paschen's Law is according to [11] presented in this Figure with the parameters for:

- $A = 1130\,\mathrm{mm}^{-1} \cdot \mathrm{bar}^{-1}$
- $B = 27.4\,\mathrm{kV} \cdot \mathrm{mm}^{-1} \cdot \mathrm{bar}^{-1}$
- $\gamma = 0.025$

In this first overview differences to the Paschen's law are obvious. In the higher areas of $p \cdot d >$ 0.5 bar · mm the breakdown voltage of the PCBs seems to be slightly under the curve. A lower dielectric strength could be assumed here. In contrast to this behaviour the area of $p \cdot d < 0.25$ bar · mm of the breakdown voltage of the PCB seems to be more and more underrated by the Paschen's law. This result could lead to an assumption that a better dielectric strength is available. Would this be confirmed in further research, PCB designs could be adapted slightly within this design area.

Additionally, during repetitive measurements with these circuit board a dependence of the breakdown voltage regarding previous breakdowns on this board are observed. A permanent influence on the PCB material can be deduced, thus a breakdown leads to a damaged PCB with undefined properties. Resulting in the need of a change of PCBs with a single breakdown occurrence with no exceptions.

VIII Conclusion

The paper describes an investigation of creepage distances on printed circuit boards induced by DC voltages. This study in the article is one of the upcoming insulation coordination studies for power electronic devices in aircraft applications. For upcoming life time testing loaded by rectangular stress, this investigation delivers a first understanding of the environmental conditions' influence on creepage distances. This study offers experiment-driven investigations, the d-optimal design is presented, the test bench is explained, and the results are discussed in detail.
It presents a mathematical model of the creepage distance dependent on climate parameters and analyses the goodness of fit. A confidence interval of 98 % offers trustable results. One measurement point for climate test in the experimental matrix takes 40 minutes; therefore, a further increase in the number of experiments isn't practical. Life time testing loaded by rectangular stress is more critical.
Additionally, the dependency of pressure tests are investigated and the correlation with Paschen's law are discussed. The breakdown voltage is affected by the distance, the temperature, the humidity and the pressure. The most likely effect next to the distance of the electrodes is the pressure. However, as seen in the presented data, each environmental condition has an influence and thus the interaction of these influences should be researched carefully. Especially because they occur simultaneously during the application and could be system critical.
The environmental condition is crucial for isolation coordination for a power electronic device for aviation applications. This paper shows mathematical models based on breakdown tests on PCBs due to an applied DC voltage. Therefore, proven power electronic housing concepts with a particular focus on the temperature are required because the temperature has the lowest impact of all investigated factors. Integrated solutions without totally encapsulated housing (for example, propulsor, electrical machine, power electronic inverter) must consider the challenging environmental conditions at their mounting location. Nevertheless, the time and the fast-changing voltage shapes are other exciting parameters. After this experience has been gained, design recommendations for power-dense power electronic components can be developed.

References

[1] H. Schefer, L. Fauth, T. H. Kopp, R. Mallwitz, J. Friebe and M. Kurrat, "Discussion on Electric Power Supply Systems for All Electric Aircraft," in IEEE Access, vol. 8, pp. 84188-84216, 2020. https://doi.org//10.1109/ACCESS.2020.2991804

[2] R. Foley, R. Nagappala, G. Ressler, P. Andres, B. Martel, "Application of Insulation Standards to High Voltage Automotive Applications", ISSN: 0148-7191, e-ISSN: 2688-3627. https://doi.org/10.4271/2013-01-1528 Published April 08, 2013 by SAE International in United States

[3] Audio/video, information and communication technology equipment - Part 1: Safety requirements, IEC 62368-1:2018, Oct. 2018.

[4] Q. Zhou, M. Wen, T. Xiong ,T. Jiang, M. Zhou,X. Ouyang and L. Xing,"Study on Insulation Breakdown Characteristics of Printed Circuit Board under Continuous Square Impulse Voltage", Energies 2018, 11(11), 2018. https://doi.org/10.3390/en11112908

[5] W. Li, I. Cotton and R. Lowndes, "Development of a Test Method for Validation of Creepage Distances in High Voltage Aerospace Power Systems," 2020 IEEE Electrical Insulation Conference (EIC), 2020, pp. 517-520, https://doi.org/10.1109/EIC47619.2020.9158720.

[6] Y. Gao, Y. K. Men and B. X. Du, "Effect of relative humidity on surface dielectric breakdown of epoxy based nanocomposites under repeated pulses," Proceedings of 2014 International Symposium on Electrical Insulating Materials, 2014, pp. 69-72, https://doi.org/10.1109/ISEIM.2014.6870722.

[7] International Standard Atmosphere, DWD, Access: 05.12.21. http://www.iup.uni-bremen.de/emerge/home/pressure_altitude.html

[8] C. Sun and C. Lu, "Design and Development of an Experimental Design and Evaluation System", 2014 Fourth International Conference on Instrumentation and Measurement, Computer, Communication and Control, 2014, pp. 175-179. https://doi.org//doi:10.1109/IMCCC.2014.44
[9] P.F. de Aguiar, B. Bourguignon, M.S. Khots, D.L. Massart, R. Phan-Than-Luum, "D-optimal designs Chemometrics and Intelligent Laboratory Systems", Volume 30, Issue 2, 1995, Pages 199-210. https://doi.org/10.1016/0169-7439(94)00076-X
[10] Environmental Conditions and Test Procedures for Airborne Equipment, EUROCAE ED-14F, 2008. https://do160.org/rtca-do-160g/
[11] A. Kuechler, "High Voltage Engineering", Schweinfurt, Germany: Springer Vieweg, 2018.